doi:10.14311/ppt.2025.1.28
Plasma Physics and Technology **12**(1):28–33, 2025

MODELLING OF SWITCHING ARCS AT SHORT ELECTRODE DISTANCES

S. Gortschakow*, R. Methling, D. Gonzalez

Leibniz Institute for Plasma Science and Technology, Felix-Hausdorff-Straße 2, 17489 Greifswald, Germany

* sergey.gortschakow@inp-greifswald.de

Abstract. Properties of the arc plasma at electrode distances below 1 mm have been studied by one-dimensional time-dependent (1D-t) fluid-Poisson model. Silver vapour is assumed to be the arc medium, as the electrodes mainly contain Ag. Pronounced voltage falls in the near-electrode regions were found. The model predicts clear thermal non-equilibrium as well as negative anode fall in case of small DC currents. For implementation in power grids simulations, a simplified arc model in form of current – voltage characteristics was derived. Predicted modelling results for electrical characteristics at various conditions have been compared with experimental results obtained for a low-voltage DC hybrid switch. A reasonable agreement between predicted and measured data was found.

Keywords: fluid simulations, arc plasma, non-equilibrium plasma, microarc.

1. Introduction

Increasing market of DC loads and sources like electrical vehicles batteries, solar power modules, lighting and data centres, requires implementation of new power control devices and safety management systems, like e.g. DC circuit breakers. Those devices should act fast and provide secure power interruption especially in case of emergency owing the difficulties of switching DC currents. Hybrid switching devices combine advantages of short reaction times of power electronics and the galvanic disconnection of mechanical switches with moving electrodes and are, therefore, the most promising solution for electrical energy management for battery electrical vehicles and low voltage power grids as well. In order to optimize the design and operation conditions of those switches a detailed understanding of physical processes related to the arc is needed. The peculiarity of this specific switching process is a very short electrode distance, which is typically below 1 mm at the end of the interruption sequence. The knowledge of switching arc characteristics during the arcing phase up to the instant of current termination allow for a right choice of switching sequence timing in order to avoid arc re-ignition.

In the present contribution the results of a numerical study of an arc discharge with moving electrodes at short electrode distances are presented. The arc plasma was modelled using an advanced fluid approach with a corresponding fluid–Poisson solver [1, 2] using the equation system [3]. Based on the discharge geometry and boundary conditions, a one-dimensional, metal vapour dominated plasma was studied. Plasma characteristics, as well as the electrical data have been calculated for the active phase (DC) and for the decaying plasma during switching off phase up to the current interruption. Based on the obtained parameters a current – voltage characteristics was derived, which can be used as a simplified arc model.

2. Brief description of the model

The model was derived taking into account the following assumptions. The arc is dominated by the metal vapour, which is produced by contact bridge explosion during the initial contact separation phase [4]. In the experiments [5], $AgSn_2O$ contact pieces have been used which is a typical contact electrode material in low voltage switching devices. Analysis of emission spectra has shown that the arc plasma consists of 91–96% Ag, and 4–9% Sn_2 [5, 6]. No detectable contributions associated with air, like e.g. radiation of Hydrogen or Nitrogen were found. The plasma structure is dominated by the axial direction, while the radial profiles of all relevant properties have been assumed to be homogeneous. This assumption is acceptable when the radial dimensions of the plasma are larger than the axial ones [3]. Experiments [5] have shown arc diameters estimated from emission spectra of 1–6 mm, while the contact distance was in the range of 20–800 µm. Commutation of power electronics within hybrid switching devices takes typically less than 10 µs. In the case of fast fault detection the arcing phase will be at the same order of magnitude. At such conditions, the movement of the electrodes might be neglected. In real applications, however, the arcing time might be much longer, up few hundreds of microseconds. Simulations have been performed, therefore, for two different situations - for the set of fixed electrode distances and including the electrode movement. Separate model which include the electrode cooling after current termination was applied for study of plasma decay. Following experimental conditions [5, 6], the electrode separation velocity was set to 1 m/s.

The values of DC arc voltage were chosen according to the measurements [5]. Within the current range of interest, the arc voltage set between 0.5 and 30 V at estimated electrode distances of 20–800 µm. This voltage provides the current density

Nr	reaction	reference
1	$Ag + e \rightarrow Ag + e$	[11]
2	$Ag + e \rightarrow Ag(5p^2P^0_{1/2}) + e$	[11, 12]
3	$Ag + e \rightarrow Ag(5p^2P^0_{3/2}) + e$	[13]
4	$Ag + e \rightarrow Ag(6p^2P^0_{1/2}) + e$	[13]
5	$Ag + e \rightarrow Ag(6p^2P^0_{3/2}) + e$	[13]
6	$Ag + e \rightarrow Ag^+ + 2e$	[14, 15]
7	$Ag^+ + e \rightarrow Ag(^*)$	[10]
8	$Ag^+ + 2e \rightarrow Ag + e$	[10]

Table 1. Plasma-chemical reactions considered in the model.

in the range $10^3 - 4 \times 10^9$ A/m^2, (current range about $10^{-4} - 10^3$ A). Initial electrode surface temperature corresponds to the boiling point of Ag (2483 K). Initial density after bridge explosion is of the order of 10^{25} m^{-3} [7].

In the decay phase the current in the mechanical switch drops down very fast. During this phase, the heat flux from the arc to the electrodes is terminated and the surface temperature decreases. This phase was considered by a separate model which takes into account the heat balance of the electrode. In order to have a realistic description of cooling dynamics, two typical temperature distributions within the electrode body have been considered (see Section 3.3 for details).

Plasma composition was assumed to be dominated by silver atoms (Ag), single ionized silver ions (Ag^+), and electrons (e). The set of plasma-chemical reactions includes elastic collisions, electron excitations, ionisation and recombination (Table 1). The rate coefficients for electron-atom collisions as well as the electron particle and energy transport coefficients [1] have been obtained from the solution of Boltzmann equation in a two-term approximation [8] in dependence on the gas temperature and mean electron energy. The data for the ion mobility and diffusion coefficients were calculated using an approach presented in [9]. Recombination kinetics was described according to [10].

Since the electrodes are the source of silver atoms, the heat balance of the electrodes has been included into the model. The heat fluxes on the boundary between the electrodes and the plasma have been described by the model similar to [16]. The flux of neutral vapour has been determined for each electrode form the surface temperature according to saturated pressure curve from [17].

3. Results and discussion

3.1. Model predictions for DC arcs

Figure 1 shows the distribution of particle densities of plasma species in the case of the shortest electrode distance of 20 µm and an arc voltage of 10 V. The ionisation degree is still below 5%. Despite a rather

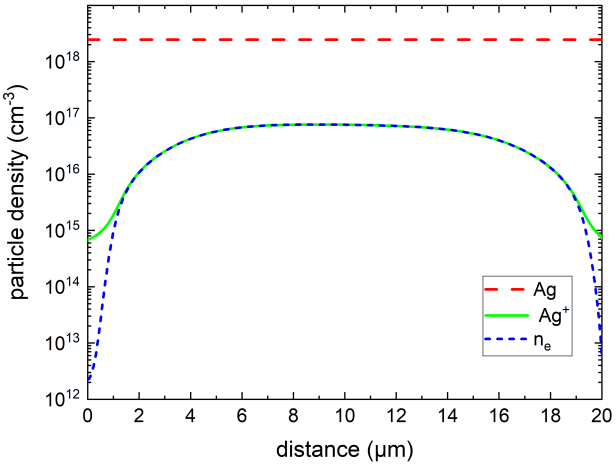

Figure 1. Axial distribution of species densities for a DC Ag arc with fixed electrode distance of 20 µm. Current density 10^7 A/cm^2. Cathode at 0 µm.

short electrode separation, the model indicates that an arc column is already present. Due to missing ionisation equilibrium, the space charge zones are formed near both electrodes. The width of the cathode layer is about 1.5 µm, while that of the anode layer is about 0.5 µm.

Pronounced differences in ion and electron densities near electrodes cause the formation of cathode and anode fall (Fig. 2). The voltage fall at the cathode is higher than the applied voltage and arises to about 20 V. An excess in the electron flux produced inside the arc column is compensated by a negative anode fall, which is of the order of 10 V in presented case. For higher electrode distances both the cathode and the anode fall become smaller. In the case of 10 V arc at 100 µm distance the cathode fall was about 12 V and the anode fall about 2 V. In general, a negative anode fall was obtained for majority of considered cases. The value of the anode fall, however, diminishes for the cases of higher applied voltage (Fig. 3) or longer electrode distances (Fig. 4). An increase of applied voltage from 2 to 6 V causes a diminution of anode fall by a factor of two (Fig. 3). In the case of increasing electrode distance, the anode fall completely disappears at $d = 800$ µm (Fig. 4).

Axial temperature profiles for electrons and heavy species are shown in Fig. 5. Clear deviation from thermal equilibrium can be seen. Due to very short gap, the energy transfer in elastic collisions is not sufficient to heat the heavy species up to temperatures comparable to that of the electrons. Even for the highest current considered, the gas temperature remains below 10000 K (Fig. 6), while the electron temperature in the column amounts to about 20000 K.

Figure 7 shows the dependence of the arc current on the arc length in the case of a fixed arc voltage. Presented behaviour is typical for arcs with conventional electrode distances, i.e. when the current is fixed, higher arc voltage for longer arc length is

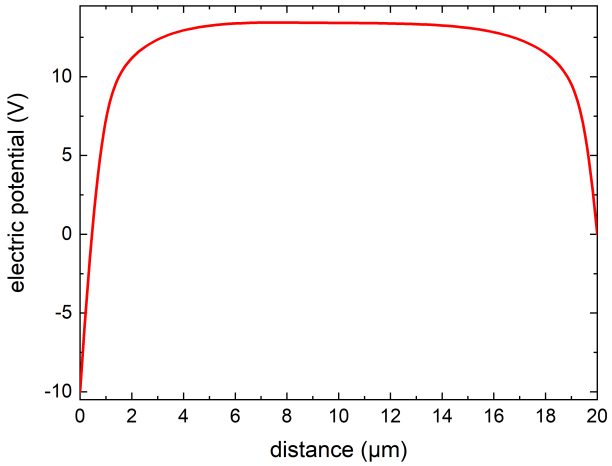

Figure 2. Electric potential distribution inside a DC Ag arc. Same conditions as in Fig. 1.

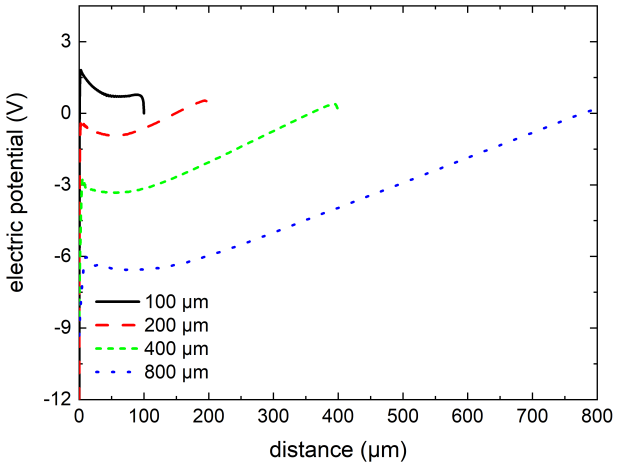

Figure 4. Electric potential distribution inside a DC Ag arc at 12 V applied voltage with moving electrodes.

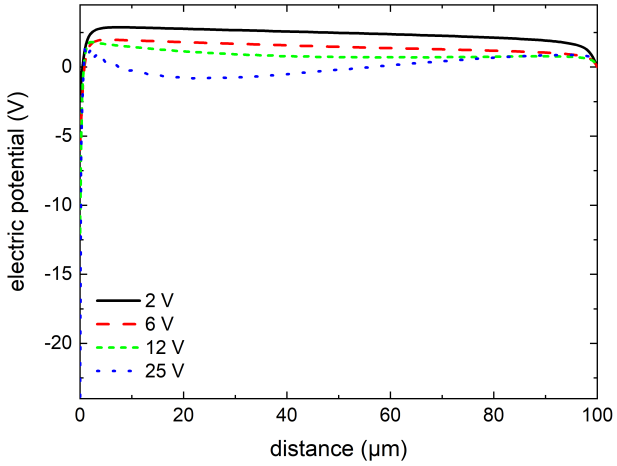

Figure 3. Electric potential distribution inside a DC Ag arc at various applied voltage and fixed electrode distance of 100 μm.

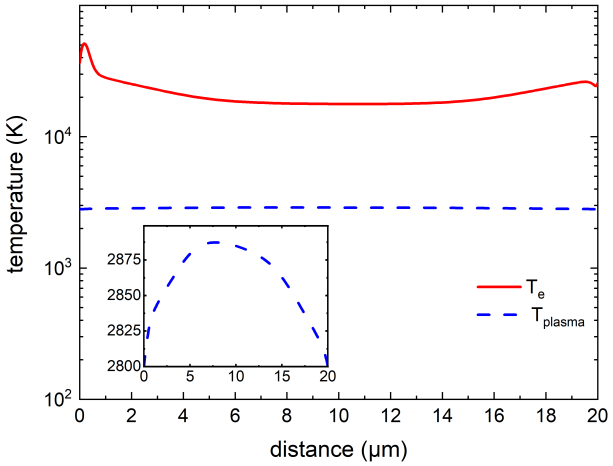

Figure 5. Axial temperature distributions of the electrons (T_e) and heavy particles (T_{plasma}). Same conditions as in Fig. 1. The inset shows heavy particle temperature in linear scale.

required. The current falls down when the electrode distance increases for fixed arc voltage and electrode surface temperature. That means that even in the case when the electrodes are still hot and, hence, provide a substantial electron emission, the arc can be terminated when the gap is large enough.

The full physical models are complex and still require an immense computation time. Therefore, simplified models like e.g. for power network simulations are desired. A simple approach is to consider the arc as a non-linear resistance or to take into account the voltage-current characteristics. An example of dependency of arc current on applied voltage for a 100 μm arc at fixed electrode temperature of 2483 K is presented in Fig. 8 . An increase in arc current results in a higher arc voltage. This is not surprising, since the considered plasma shows strong deviations from equilibrium state (cf. Fig. 5). At higher current an amount of electric energy which is necessary for the gas heating increases, causing higher voltage for maintenance of the current. Figure 9 shows the voltage-current characteristics at variable electrode distance and fixed electrode temperature. The dependency of arc voltage on the current is strongly non-linear. At lowest current values for fixed electrode distance a steep increase of the arc voltage is predicted. The steepness of $U(I)$ course decreases when the current becomes higher. Longer electrode distances require higher arc voltage for fixed current value. Corresponding curves can be calculated for various electrode temperatures and used then in form of tables for prediction of the switch resistance within the network simulations.

3.2. Model predictions for arc decay phase

Simulations with electrode movement have clarified that an arc extinction benefits from the lowering of the electrode surface temperature. Decreasing current causes a lowering of heat flux toward the electrodes, leading to surface cooling in comparison with DC phase. Resulting surface temperature

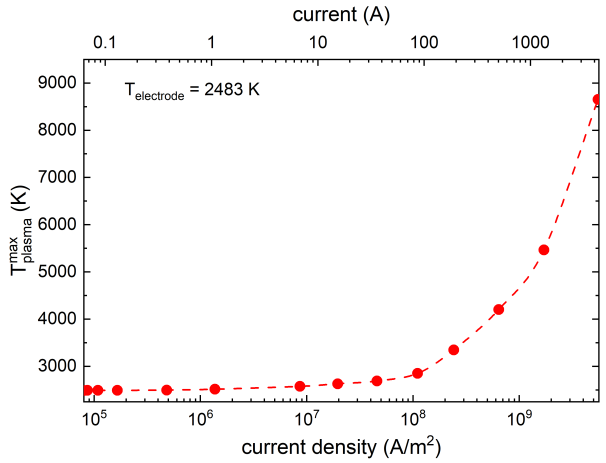

Figure 6. Maximum gas temperature T^{max}_{plasma} in dependence on the arc current for a 100 µm gap.

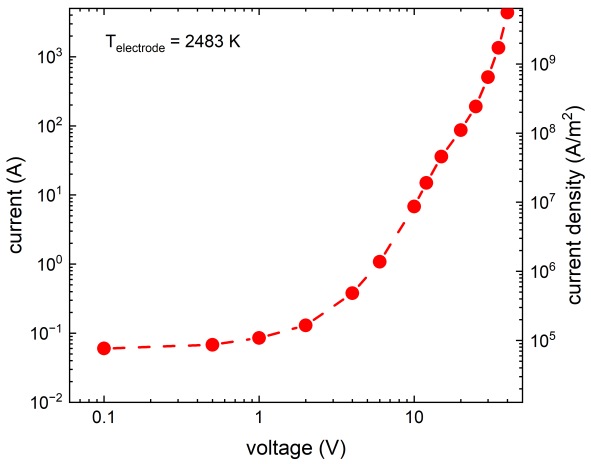

Figure 8. Dependency of the arc current on the voltage for a DC Ag arc with fixed electrode distance of 100 µm.

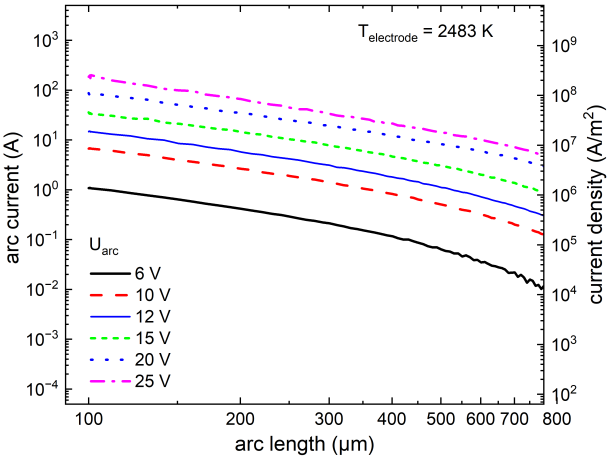

Figure 7. Dependence of the DC arc current on the electrode distance at fixed arc voltage. Opening velocity 1 m/s.

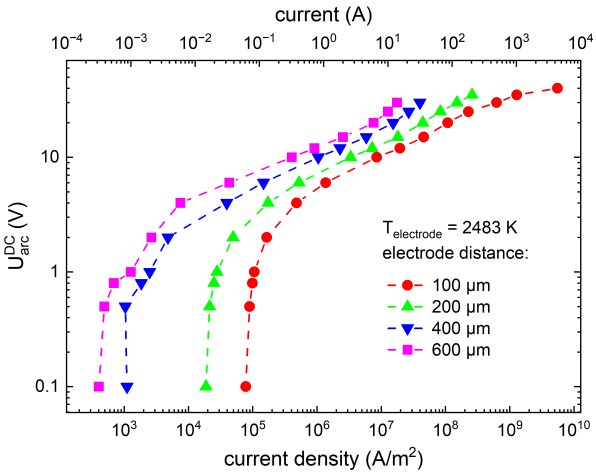

Figure 9. Voltage-current characteristics of a DC Ag arc with variable electrode distance.

depends, however, also on the depth of molten electrode material. Depending on incoming heat flux from the arc and arc duration, different molten depth and temperature profiles inside the electrode occur. Figure 10 presents two typical electrode temperature profiles. Profile 1 appears usually in the case of long arc duration in combination with moderate heat flux. It is characterised by a significant amount of melted material close to the electrode surface (assumed to be as thick as 100 µm) and linear temperature decrease toward the electrode basement. Another limiting case is a sublimation profile (profile 2). This type of profiles appears when incoming heat flux is high enough for direct vaporization of solid material, like e.g. shortly after the molten bridge explosion during contact separation. The heat penetrates inside the material only by few dozen of micrometers (10 µm in present simulations). The temporal voltage profile in the decaying phase was aligned to experimental data [6]. According to those experiments, the power electronics path of hybrid switch overtakes the whole current within about 10 µs from the mechanical switch path. The change of current path leads to a voltage drop over the contacts of mechanical switch from initial value (10–30 V) to the typical value of power electronics junctions (1–2 V). Resulting resistance of decaying arc plasma is shown in Fig. 12. In the case of sublimation profile (profile 2) the resistance increases by almost four orders of magnitude within few microseconds. Stronger electrode heating, like e. g. in case of profile 1 leads to increase of this time by a factor of 20. Therefore, shorter arc duration (i.e. fast interruption) is of advantage for successful arc termination.

3.3. Comparison with experiments

Validation of the model results have been performed by comparison with electrical characteristics of switching arc in a low-voltage hybrid switch developed in the project [6]. Its mechanical part contains two $AgSn_2O$ contact pieces with 5 mm diameter and 1 mm height. A linear motor drive provided the mean opening

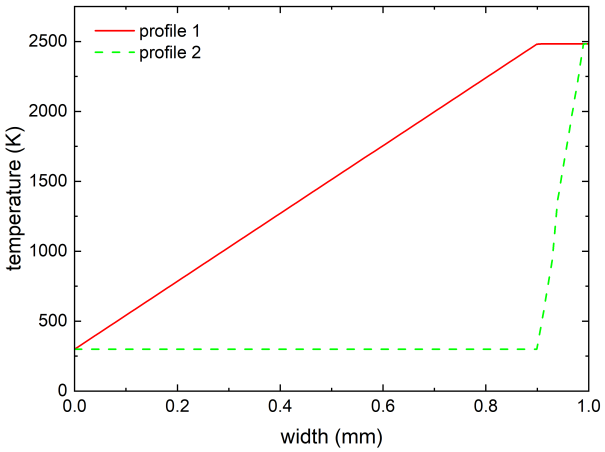

Figure 10. Assumed profiles of temperature distribution inside the electrode.

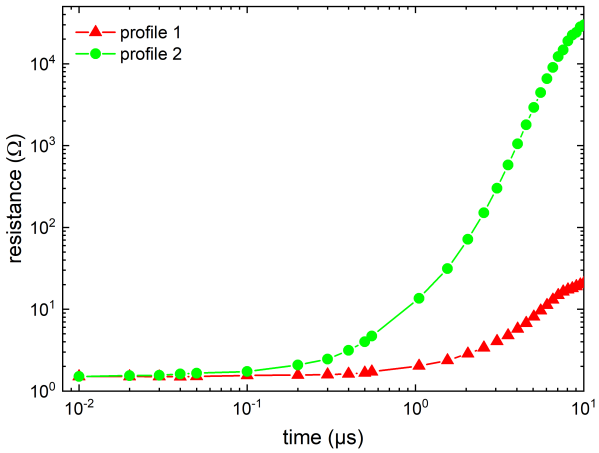

Figure 12. Arc resistance during switching off phase of hybrid device.

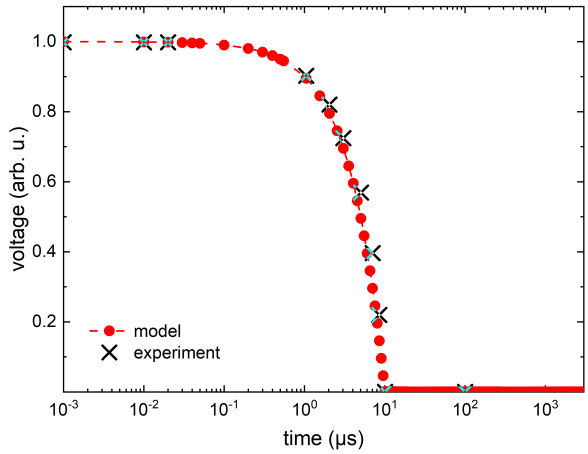

Figure 11. Voltage shape during switching off phase of hybrid device. Crosses - values from experiment, dots - assumed profile in the model.

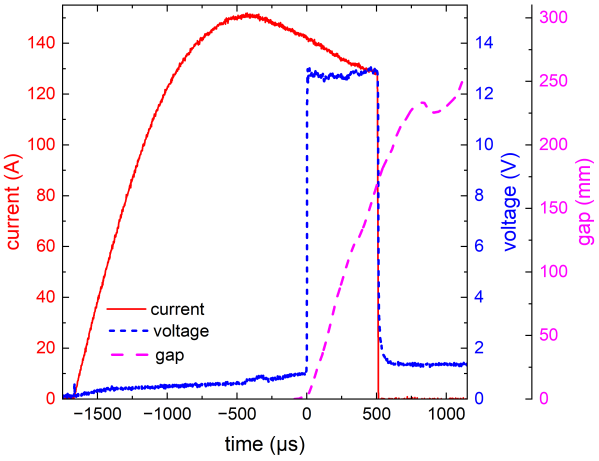

Figure 13. Example of arc current (red full line), arc voltage (blue short-dashed line) and gap distance (magenta dashed line) in a hybrid switch [6]. Mean current 150 A.

velocity of about 1 m/s. The load current between 30 and 300 A was used in experiments. An example of arc current, arc voltage and electrode distance (gap) evolution in the case of current of 150 A (mean value) and arc duration of about 500 μs is presented in Fig. 13. The time axis is shifted to the instant of arc ignition. At the instant of 500 μs, the power electronics takes the current over within about 10 μs (cf. Fig. 11). The residual voltage of ca 1.6 V corresponds to the voltage fall over electronic part. Measured arc voltages during the arcing phase were in the range 11–22 V.

Figure 14 shows the comparison of calculated arc current density during arcing phase with the data evaluated from the experiment. The error bars for experimental values result from uncertainties in estimation of arc diameter which were assumed to be as high as 25%. Shorter arc length corresponds to shorter arc duration. The data are in good agreement.

Comparison for electric characteristics during the switching off phase is presented in Fig. 15. A reasonable agreement between predicted and measured data was found.

4. Conclusions

Properties of the arc plasma at short electrode distances have been studied by means of a 1D-t fluid-Poisson model. The arc medium was a silver vapour. The model predicts a pronounced cathode voltage fall, which typically exceeds the arc voltage. The difference is compensated by a negative anode fall. In general, a negative anode fall was obtained for majority of considered cases. The model predicts strong deviations from an equilibrium state. Even for the highest current/ current density, the gas temperature was far below of that of the electrons. An increase of the electrode distance at fixed arc voltage causes strong diminishing of the arc current even for the cases when the cathode provides sufficient emission current.

For implementation in power grids simulations a simplified arc model in form of current – voltage

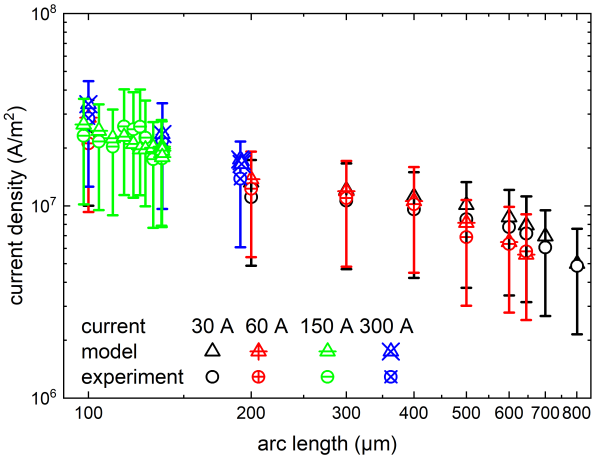

Figure 14. Comparison between measured and predicted current density for Ag arcs with variable electrode distance during the arcing phase.

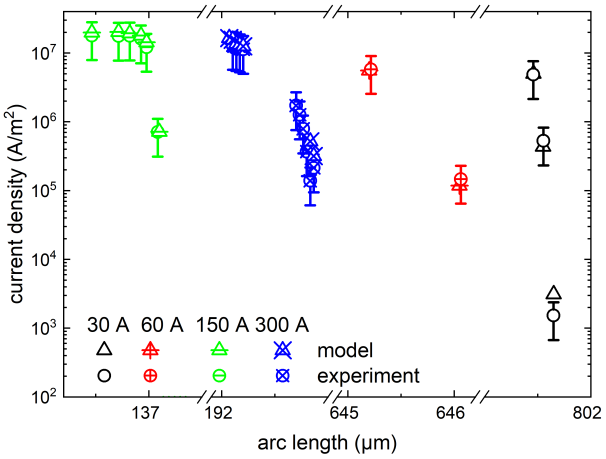

Figure 15. Comparison between measured and predicted current density for Ag arcs with variable electrode distance during switching off (decay phase).

characteristics was derived. At a fixed electrode distance, a voltage increase will cause a growth of the arc current. This fact has to be taken into account for optimization of electrode opening velocity and maximum contact distance in hybrid switches.

The model was verified by comparison with electric characteristics measured in a low-voltage DC hybrid switch. A reasonable agreement between those data was found.

Acknowledgements

This work was founded by German Federal Ministry for Economic Affairs and Climate Action – BMWK within the framework of the "AutoHybridS" project, funding reference Nr. 03EI606D.

References

[1] M. M. Becker and D. Loffhage. Enhanced reliability of drift-diffusion approximation for electrons in fluid models for nonthermal plasmas. *AIP Advances*, 3:012108, 2013. doi:10.1063/1.4775771.

[2] M. M. Becker and D. Loffhage. Derivation of moment equations for the theoretical description of electrons in nonthermal plasmas. *Adv. Pure Math.*, 3:343–352, 2013. doi:10.4236/apm.2013.33049.

[3] M. Baeva and D. Uhrlandt. Characterisation and application of direct current microarcs: a review. *J. Phys. D: Appl. Phys.*, 58:263001, 2025. doi:10.1088/1361-6463/ade44d.

[4] J. Swingler and A. Sumpton. Arc erosion of $AgSnO_2$ contacts at different stages of a break operation. *Rare metals*, 29:248–254, 2010.

[5] D. Gonzalez, R. Methling, S. Gortschakow, et al. Plasma of a dc hybrid-switch at beginning of contact separation. *Proc. IEEE 67th Holm Conference on Electrical Contacts, Tampa, FL, USA*, 29:1–6, 2022. doi:10.1109/HLM54538.2022.9969827.

[6] X. Guo, F. Schilling, F. Berger, et al. Autonom gesteuerter Hybridschalter mit effizienter Wiederverfestigungsdetection (abschlussbericht). arXiv:https://www.tib.eu/de/suchen/id/TIBKAT:1925509745/Verbundvorhaben-AutoHybridS-Autonom-gesteuerter?cHash=2322cefc788feb0c66d1a33aa6672ae5.

[7] M. Hu and B. R. Kusse. Experimental measurement of Ag vapor polarizability using optical interferometry and x-ray radiography. *Phys. Rev. A*, 66(6):062506, 2002. doi:10.1103/PhysRevA.66.062506.

[8] T. Bräuer, S. Gortchakov, D. Loffhagen, et al. The temporal decay of the diffusion-determined afterglow plasma of the positive column. *J. Phys. D: Appl. Phys.*, 30(23):3223–3239, 1997. doi:10.1088/0022-3727/30/23/007.

[9] P. Porytsky, I. Krivtsun, V. Demchenko, et al. Transport properties of multicomponent thermal plasmas: Grad method versus Chapman-Enskog method. *Phys. Plasmas*, 20(2):023504, 2013. doi:10.1063/1.4790661.

[10] Y. P. Raiser. *Gas Discharge Physics*. Springer-Verlag Berlin, 1991.

[11] M. Baeva. Electron collision cross-sections for Silver (private communication).

[12] NIST. NIST Electron Elastic-Scattering Cross-Section Database. [2024-06-24]. doi:10.18434/T4NK50.

[13] W. Lochte-Holtgreven. *Plasma diagnostics*. North-Holland publishing company, Amsterdam, 1968.

[14] R. S. Freund, R. C. Wetzel, R. J. Shul, et al. Cross-section measurements for electron-impact ionization of atoms. *Phys. Rev. A*, 41(7):3575–3595, 1990. doi:10.1103/PhysRevA.41.3575.

[15] D. Gupta, R. Naghma, and B. Antony. Electron impact total and ionization cross sections for Sr, Y, Ru, Pd, and Ag atoms. *Can J. Phys.*, 91(9):744–750, 2013. doi:10.1139/cjp-2013-0174.

[16] M. Baeva, R. Kozakov, S. Gorchakov, et al. Two-temperature chemically non-equilibrium modelling of transferred arcs. *Plasma Sources Sci. Technol.*, 21(5):055027, 2012. doi:10.1088/0963-0252/21/5/055027.

[17] M. B. Panish. Vapor Pressure of Silver. *Chem. Eng. Data*, 6:592–594, 1961.